Published in final edited form as:
Neurosurgery. 2007 December ; 61(6): 1305–1313. doi:10.1227/01.NEU.0000280168.25968.49.

QUANTIFICATION OF HEMODYNAMIC CHANGES INDUCED BY VIRTUAL PLACEMENT OF MULTIPLE STENTS ACROSS A WIDE-NECKED BASILAR TRUNK ANEURYSM

Minsuok Kim, Ph.D.,
Department of Mechanical and Aerospace Engineering, University at Buffalo, State University of New York, Buffalo, New York

Toshiba Stroke Research Center, School of Medicine and Biomedical Sciences, University at Buffalo, State University of New York

Elad I. Levy, M.D.,
Departments of Neurosurgery and Radiology, University at Buffalo, State University of New York, and Millard Fillmore Gates Hospital, Kaleida Health, Buffalo, New York

Toshiba Stroke Research Center, School of Medicine and Biomedical Sciences, University at Buffalo, State University of New York

Hui Meng, Ph.D., and
Departments of Mechanical and Aerospace Engineering and Neurosurgery, University at Buffalo, State University of New York, Buffalo, New York

Toshiba Stroke Research Center, School of Medicine and Biomedical Sciences, University at Buffalo, State University of New York

L. Nelson Hopkins, M.D.
Departments of Neurosurgery and Radiology, University at Buffalo, State University of New York, and Millard Fillmore Gates Hospital, Kaleida Health, Buffalo, New York

Toshiba Stroke Research Center, School of Medicine and Biomedical Sciences, University at Buffalo, State University of New York

Abstract

OBJECTIVE—The porous intravascular stents that are currently available may not cause complete aneurysm thrombosis and may therefore fail to provide durable protection against aneurysm rupture when used as a sole treatment modality. The goal of this study was to quantify the effects of porous stents on aneurysm hemodynamics using computational fluid dynamics.

METHODS—The geometry of a wide-necked saccular basilar trunk aneurysm was reconstructed from a patient′s computed tomographic angiography images. Three commercial stents (Neuroform2; Boston Scientific/Target, San Leandro, CA; Wingspan; Boston Scientific, Fremont, CA; and Vision;

Reprint requests: Elad I. Levy, M.D., University at Buffalo Neurosurgery, 3 Gates Circle, Buffalo, NY 14209. Email: elevy@buffns.com.

Disclosures

L. Nelson Hopkins, M.D., receives industry grant support from Boston Scientific, Cordis, and Micrus; is a stock- or shareholder in Boston Scientific, EndoTex, and Micrus; receives consultant fees from Abbott, Bard, Boston Scientific, Cordis, EndoTex, and Micrus; and holds a board, trustee, or officer position for Access Closure, marketRX, and Micrus. Elad I. Levy, M.D., receives industry grant support and honoraria from Boston Scientific and Cordis; and has received carotid stent training from Abbott Vascular and ev3; and patent royalties from Zimmer Spine.

Guidant Corp., Santa Clara, CA) were modeled. Various combinations of one to three stents were virtually conformed to fit into the vessel lumen and placed across the aneurysm orifice. An unstented aneurysm served as a control. Computational fluid dynamics analysis was performed to calculate the hemodynamic parameters considered important in aneurysm pathogenesis and thrombosis for each of the models.

RESULTS—The complex flow pattern observed in the unstented aneurysm was suppressed by stenting. Stent placement lowered the wall shear stress in the aneurysm, and this effect was increased by additional stent deployment. Turnover time was moderately increased after single- and double-stent placement and markedly increased after three stents were placed. The influence of stent design on hemodynamic parameters was more significant in double-stented models than in other models.

CONCLUSION—Aneurysm hemodynamic parameters were significantly modified by placement of multiple stents. Because the associated modifications may be helpful as well as harmful in terms of rupture risk, use of this technique requires careful consideration.

Keywords

Aneurysm; Endovascular; Hemodynamics; Multiple stenting; Stent

---

Microsurgical and endovascular techniques for cerebral aneurysm treatment have improved over the last few decades. However, very wide-necked and fusiform aneurysms provide considerable difficulties to neurosurgeons because they are not amenable to conventional coil embolization or surgical approaches (30).

Presently, porous stents are used commonly in the management of these difficult cerebral aneurysms to provide a scaffold across the aneurysm neck, which is followed by packing of the aneurysm sac with detachable coils delivered through the stent struts (3,22). Investigators (14,16) have reported that stent-alone treatment can alter aneurysm hemodynamics and create favorable flow conditions by inducing thrombosis, which excludes the aneurysm from the cerebral circulation. However, the results of stenting without additional coil embolization to induce immediate or permanent aneurysmal occlusion have been inconsistent (15,16,29).

Recent reports have shown that the placement of multiple stents across the aneurysm neck improves the efficiency of stenting by reducing the permeability of aneurysmal inflow overall. Doerfler et al. (7) used a double-stent method to treat small, wide-necked aneurysms of the vertebral artery in two patients. In each patient, marked reduction of aneurysm flow was observed by angiography, and complete occlusion was obtained after 7 days. On the basis of this anecdotal clinical report, Cantón et al. (3) performed a study to quantify the hemodynamic changes induced by sequential placement of stents. These investigators measured the two-dimensional pulsatile velocity field within a flexible silicone sidewall aneurysm model using digital particle image velocimetry. The reduction of maximum averaged velocity, vorticity, and shear stress induced by placing the first stent was remarkable. Reductions in these quantities were less pronounced after a second or third stent was placed.

In this study, our objectives were to quantify and characterize the variations of hemodynamic parameters thought to be important in aneurysm pathogenesis and thrombosis through sequential virtual placement of stents across the aneurysm neck. Using computational fluid dynamics (CFD) and angiographic image analysis, we compared the effects of three porous, commercial stent designs on aneurysm hemodynamics.

MATERIALS AND METHODS

Aneurysm Geometry Reconstruction

A basilar artery aneurysm in a 67-year-old woman was selected as a reference for computer modeling in this study. This aneurysm was a wide-necked basilar trunk aneurysm that was 3.7 by 6.2 mm in size. For CFD analysis, the geometric dimensions of the aneurysm and its parent vessel were reconstructed from computed tomographic angiography images composed of 512 by 512 pixels with a 153 mm^2 field of view (Fig. 1). The resolution between planes was 0.4 mm. During the geometry reconstruction process, bone detail was subtracted, and the resulting vascular structure was segmented and smoothed for rendering.

Stent Geometry

The reconstructed aneurysm was virtually treated with one, two, or three stents. Three different stents, an intracranial self-expanding Neuroform2 stent (2.0 × 20 mm; Boston Scientific/Target, San Leandro, CA), a coronary balloon-mounted Vision stent (2.0 × 12 mm; Guidant, Santa Clara, CA), and an intracranial self-expanding Wingspan stent (2.0 × 20 mm; Boston Scientific, Fremont, CA), were modeled by use of computer-assisted design software (ProEngineer; PTC, Needham, MA) (Fig. 2). The strut sizes (metal width of the strut) are as follows: Neuroform2, 65 μm; Vision, 60 μm; and Wingspan, 70 μm. The stent porosities (the percentage of total stent wall area that is fenestrated) are 83.4% for the Neuroform2, 88.5% for the Vision, and 79.6% for the Wingspan. The stents were virtually conformed to fit into the parent vessel lumen and virtually deployed across the aneurysm neck. We modeled an unstented aneurysm and a series of stented aneurysms, as listed in Table 1. For multiple-stent models, two scenarios were considered. In the optimal scenario, the struts of the additional stents evenly divided the openings of the first stent; whereas in the suboptimal scenario (Model N2-p), the additional stent was minimally shifted from the first one. Geometries of the unstented, single-, double-, and triple-stented aneurysm models are shown in Figure 3.

Computational Fluid Dynamics Modeling

Computational grids consisting of approximately 600,000 to 4.8 million tetrahedral elements with 0.3-mm maximum element size were created for the unstented and stented models with ICEM CFD software (Ansys, Berkeley, CA). These grids were imported into a finite volume-based CFD code, Star-CD (CD-Adapco, Melville, NY), to solve the Navier-Stokes equations with a second-order accuracy scheme. Velocity and pressure fields were computed under the assumptions of incompressible, laminar, steady-state flow and Newtonian fluid dynamics. The Reynolds number, a nondimensional fluid dynamic similarity parameter, was 362, which is in the range of normal arterial flow conditions in the cerebrovascular circulation. The viscosity and density measurements of blood used in the simulations were 0.0035 m·s and 1056 kg/m^3, respectively.

Hemodynamic Parameters

To illustrate the overall flow characteristics of the aneurysm, we plotted the velocity vectors at the midplane of the aneurysm models. Moreover, because a typical flow pattern in an aneurysm is rotational (25), the circulatory flow in the aneurysm was quantitatively illustrated by the vorticity contour plot on the midplane. To compare the influence of various stent combinations on the aneurysm wall, we calculated the elevated wall shear stress (WSS) (13). To quantify stasis of flow in the aneurysm, we calculated the turnover time. The turnover time was defined as the aneurysm volume divided by the aneurysmal inflow rate.

RESULTS

From the velocity vectors plotted to visualize aneurysmal flow patterns, two distinct vortices were observed in the unstented aneurysm (Fig. 4). This complex flow pattern was dampened by stenting, even with a single stent. Detailed circulatory flow characteristics in the aneurysm are shown in Figure 5 as vorticity contours plotted on the midplane of each aneurysm model. The magnitude of the vorticity in the aneurysm dome was reduced by a stent, and additional reduction in vorticity was achieved by additional stent deployment. Although all stents attenuated vortical flow within the aneurysm, there were discernible differences in the stent effect, depending on the quality of the deployment and the design of the stent. The Wingspan stent was more effective in reducing aneurysmal vorticity than the other two stent designs in the double-stented aneurysm models.

Figure 6 shows the elevated aneurysmal WSS area (percentage) in each of the aneurysm models. In the single-stented aneurysm models (N, V, and W), the reduction of the elevated WSS area was insignificant (<10%). There was no substantial difference associated with stent design in these single-stented aneurysms. However, the effect of stenting was significant and the effect of the stent design was evident in double-stented aneurysm models (N2, NV, and W2), except in the poor-deployment, double-stent model (N2-p). The most significant elevation in WSS area reduction (45%) effected by double stents was achieved with two Wingspan stents (W2). In triple-stented aneurysm models (N3 and N2V), the elevated WSS area was more significantly reduced by stenting, but the stent design effect was indistinct.

Figure 7 illustrates the surface contours of the low-level WSS in the aneurysm models. The aneurysmal WSS in the unstented model was above the upper limit of this low WSS level. A considerably lower WSS zone was apparent at the distal side of the aneurysm dome after single-stent placement. As the number of stents increased, WSS values at the proximal and distal sides of the aneurysm dome were reduced. This effect was more pronounced with the Wingspan stent than with other stents in the single- and double-stented aneurysm models. The aneurysmal WSS was substantially reduced by triple stenting.

Quantification of stent-induced aneurysm hemodynamics was performed using turnover time Fig. 8. The increase in turnover time in stented aneurysm models was unremarkable compared with that in the unstented aneurysm model (1.2 to 1.3 times longer in stented than unstented models). A greater increase in turnover time, however, was obtained by double stenting (1.4 to 1.8 times longer than in unstented models). Significant stent design dependency was found only among the double-stented models. A turnover time of approximately

DISCUSSION

Aneurysmal flow pattern is a primary hemodynamic factor that shows overall flow characteristics in the aneurysm and potentially indicates further development of the aneurysm. The importance of aneurysmal flow patterns was accentuated in a recent study conducted by Cebral et al. (4). These authors found that ruptured aneurysms were more likely to have complex flow patterns, whereas simple flow patterns were associated with unruptured aneurysms. Ujiie et al. (27,28) associated secondary flow circulation, which is often found in an aneurysm with a large aspect ratio, with aneurysm rupture risk. Complex flow patterns have been thought to increase inflammatory cell infiltration in the aneurysmal wall, thereby increasing rupture risk (5,12,28). In the present study, the flow pattern in the unstented, wide-necked, basilar trunk aneurysm had two distinct vortices. This complex flow pattern was simplified and the vortices were suppressed by the placement of one to three stents. This finding indicates that stent placement in this aneurysm geometry could reduce the risk of aneurysm

rupture by dampening the aneurysmal inflow, although a single stent may not be enough to induce complete aneurysm thrombosis.

Stent-alone treatment is unpredictable, however, and the results of flow alteration, especially in conjunction with single-stent placement, may vary significantly from case to case, depending strongly on patient-specific aneurysm geometry. The placement of a single stent might result in a new, concentrated, jet-like inflow that directly impinges on the aneurysm wall. Cebral et al. (4) found that a concentrated jet is more likely to cause rupture than diffuse flow. In our recent canine model of a created bifurcation (21), we demonstrated that the hemodynamics associated with jet impingement can cause destructive remodeling of the wall and lead to the initiation of an aneurysm. It is not inconceivable that such hemodynamic conditions associated with flow impingement, if created inadvertently inside the aneurysm sac by stenting, could potentiate aneurysmal rupture. On the other hand, multiple stents can reduce the risk of forming jet-like inflow by eliminating large open pores and possibly by inducing a healing response (1,7). Hence, because of the potentially opposite outcomes after stenting, flow simulations with patient-specific aneurysm geometry may be useful for understanding stent-induced hemodynamics effects.

As mentioned, the aneurysmal flow pattern illustrates global aneurysm hemodynamics; however, the arterial wall is directly affected by near-wall hemodynamics via signal transduction of endothelial cells. For decades it has been known that WSS, a tangential drag force per unit area of endothelial surface, is an important hemodynamic parameter correlated with aneurysm growth and rupture (24,26). Prolonged high WSS is known to cause internal elastic lamina fragmentation (20) and may be responsible for cerebral aneurysm initiation (21,24). In saccular aneurysms, the distal neck region is often subject to chronically high WSS, which may be responsible for expansion of the aneurysm neck via a destructive vessel wall remodeling process similar to the initial phase of aneurysm formation (10,11). In our simulations of multiple-stent placements, the stents deflected the inflow and restrained the WSS elevation on the aneurysm wall. This result is consistent with our previous finding that stenting could lessen exposure of the distal neck to high WSS (21), thus potentially deferring further expansion of the aneurysm neck.

Different from the aforementioned high-WSS-mediated destructive remodeling pathways (10,11,20), an inflammatory and atherosclerotic pathway triggered by low WSS has also been implicated in aneurysm pathogenesis (6,21,23). Excessively low WSS (<0.4 Pa) within the aneurysm sac could lead to atherosclerotic inflammatory infiltration (19) and thereby cause deterioration of the aneurysm wall that could ultimately lead to rupture (28). From this standpoint, not all effects revealed by our study of multiple stenting on the aneurysm wall are desirable. We found that the low-WSS area in the dome of the aneurysm was increased after the placement of multiple stents. Much research in this area is needed to delineate the mechanisms for aneurysm wall deterioration and rupture and thereby clarify the role of stenting.

To afford lasting protection against rupture, an aneurysm needs to be hemodynamically excluded from the arterial circulatory system. It is expected that stents can accomplish this by stimulating aneurysmal thrombosis (17). Researchers (2,9,10) have shown that increasing aneurysmal flow turnover time (an indication of stasis) can induce thrombus formation in cerebral aneurysms. In the present study, aneurysmal inflow was consistently decreased by sequential stenting. As inflow decreases, the turnover time increases (Fig. 8) in inverse proportion, and the chance of aneurysmal thrombosis likely increases. Excessive neointimal growth on the stent surface may lead to stent-induced stenosis (2,8,9).

The potential risk of infarction or ischemia caused by a single stent compromising perforating branches may not be important (18). However, the permeability of flow through the stents

decreases as the number of stents increases. There is then a greater chance for interruption of flow into perforating branches that could potentially lead to a stroke. Therefore, careful consideration for use of single- or multiple-stenting technique is required in accordance with the patient's neu-rovascular anatomy.

CONCLUSION

The hemodynamic parameters of the patient-specific aneurysm in this study were considerably modified by the placement of multiple stents. The influence of stent design on aneurysm hemodynamics was significant in the double-stented aneurysms but less important in single- and triple-stented aneurysm models. Depending on the quality of the stent deployment in the double-stented aneurysm models, the effects of stenting on aneurysm hemodynamics were substantially different. Because the effect of stent placement on aneurysmal hemodynamics may influence rupture risk, additional studies of the biological responses to stent placement are required.

COMMENTS

In this article, Kim et al. present a computerized study of flow within an aneurysm. Using a model of a given patient′s aneurysm, they modified it with virtual placement of three different types of commercially available stents in combinations, including a single stent, a stent within a stent, and in one case, triple stents, to observe changes in flow. The concept here is straightforward. Complex flow patterns including wall shear stress, vortex formation within the aneurysm, and jets against the weakened part of the wall will affect endothelial cell proliferation, wall breakdown, possible aneurysm growth, and rupture rates. The authors understand that certain aneurysms, such as a basilar aneurysm, which they model in this article, may be difficult to treat by conventional endovascular or open-surgical methods, and they therefore wonder whether stent technology may be helpful. In this regard, they are moving away from the concept of stent-assisted coiling and instead looking at whether stents themselves will redirect flow and allow an aneurysm to thrombose or heal. Their interesting findings suggest that indeed, placement of a virtual stent within their computer′s computational fluid dynamics model will change flow. However, it is conceivable, especially when a single stent is used, that placing the stent may actually create a jet that may be harmful, and they provide a clinical example of this. The authors explain that the placement of two stents (one within the other, as long as they are not perfectly overlapping) will create a tighter meshwork that may be beneficial and that the third stent may add slight benefit.

The benefits of this approach are obvious. This model permits additional understanding of flow dynamics without endangering patients. The concerns are whether the model is accurate in life, and whether we fully understand which systems provide the ideal flow dynamics that we attempt to achieve. The authors should be questioned as to their first paragraph, where they suggest that some aneurysms are not amenable to treatment, to a more general statement that aneurysms may not be amenable to treatment, as this is often an individual debate.

The figure presentations are quite convoluted. It should be clarified that this is but one clinical example and truly a report of a methodology. Rather than establishing the methodology, this article simply introduces it. The authors also make assumptions in their mathematical model, such as that of laminar flow, which really does not occur in this basilar region that they study. Of course, the mathematical construct is necessary because it allows us to further evaluate the flow. The authors′ major strength in this article is their ability to model flow. They are encouraged to improve their presentation of data for their audience and to carefully explain the limitations of our understanding of these flow changes on vascular biology, given the relatively limited number of factors that they are studying.

Robert J. Dempsey

Madison, Wisconsin

Kim et al. have elegantly analyzed the hemodynamic effects of multiple stent placement across a wide-necked basilar aneurysm using a virtual model. In their study using computational fluid dynamics and angiographic image analysis, the authors found intra-aneurysmal flow patterns to be dampened by stenting, with reduction in vorticity being proportional to the number of stents used. Stent placement also lowered wall shear stress and average flow velocity in the aneurysm dome.

Although advancements in microsurgical and endovascular techniques have improved the treatment of cerebral aneurysms, those with wide necks or fusiform morphology continue not to be amenable to conventional therapeutic modalities. With recent investigations reporting possible beneficial effects after multiple stent placements in such cases, this article provides insight into the hemodynamic basis for these alterations. Moving forward, additional prospective studies with long-term follow-up will be important for appropriate patient selection, as clinical and radiographic results after use of this technique have demonstrated inconsistent outcomes.

Ricardo J. Komotar

E. Sander Connolly, Jr.

New York, New York

Kim et al. from the Buffalo group report the simulated effects of different currently available stents on intra-aneurysmal flow dynamics in a computer-modeled lateral basilar artery aneurysm. Different combinations of stents had different simulated effects on the computed flow dynamics. Stent geometry had more effect on hemodynamic parameters when multiple stents were used, rather than with single stent deployment.

The use of stents for flow diversion for the treatment of intracranial aneurysms has great potential. Hemodynamic factors clearly play a role in the formation, growth, and rupture of intracranial aneurysms. Therapies that address these factors, such as stents, may be useful in preventing aneurysm growth and rupture. It is also conceivable that stents might be used in the future to prevent aneurysm development. It may be possible to predict the development of aneurysms in some patients based on flow analysis of circle of Willis geometry and individual patient genomic factors.

The present study of Kim et al. illustrates both the potential of this mode of therapy as well as the present substantial limitations. We have few stents available for use in the cerebrovasculature: two are FDA approved and only one is appropriate for something similar to this indication. None are optimized for flow diversion. Future developments might include fabric coverings of different degrees of permeability that may allow flow into perforators. In addition, temporary or absorbable stents may allow healing of an aneurysm without a rigid, permanent device left in the cerebral circulation for the remaining life of the patient. Finally, stents can be used as delivery agents for bioactive materials such as drugs and growth factors.

One limitation of the present study is the applicability of this information for other, more complex aneurysm geometries. The model only analyzed the effects in a relatively simple system of a lateral wall aneurysm. Bifurcation aneurysms and their variants will pose different problems.

This study provides some real-world information that can be applied to practice today, as the analysis was limited to presently available stents. The addition of a second stent is likely to additionally reduce flow into an aneurysm, provided the stent happens to deploy in a complementary fashion to the first. The ability to control this with present technology is nonexistent.

Colin Derdeyn

Ralph G. Dacey, Jr.

St. Louis, Missouri

Kim et al. have prepared a report ″quantifying″ the hemodynamic changes induced by the virtual placement of multiple stents across a virtual aneurysm using computational fluid dynamics. This is an interesting article, but its usefulness is limited; despite the complexity, this report remains a theoretical quantification in an unreal, nonbiological world. Regardless, computer modeling does allow for an increase in our knowledge base with regard to cerebral aneurysms and their treatment, and the authors have used this technology to understand the effects of arterial stenting. The authors′ results demonstrate an additive effect on wall shear stress, aneurysm flow velocity, and turnover time with the use of multiple stents, which would theoretically decrease flow into the aneurysm and improve the durability of endovascular therapy that may or may not include coiling. These results are not surprising, as with the use of multiple porous stents, a decrease in the porous nature of the stent or scaffold is created that results in the decrease of inflow to the aneurysm. However, as the authors clearly state, this is not without risk, as a nonporous stent or a covered stent (which would be on the extreme spectrum of multiple porous stents) may compromise flow into the perforators, with disastrous results. Furthermore, covered stents are associated with increased thromboembolic complications, and similar problems may result from the use of too many porous stents.

Gavin W. Britz

Durham, North Carolina

Acknowledgments

Portions of this work were supported by National Institutes of Health Grants NS-047242 (HM), NS-43924 (MK, HM), and EB-002873 (MK, HM); and by National Science Foundation Grant BES-0302389 (MK, HM).

REFERENCES

1. Benndorf G, Herbon U, Sollmann WP, Campi A. Treatment of a ruptured dissecting vertebral artery aneurysm with double stent placement: Case report. AJNR Am J Neuroradiol 2001;22:1844–1848. [PubMed: 11733313]
2. Burleson AC, Turitto VT. Identification of quantifiable hemodynamic factors in the assessment of cerebral aneurysm behavior. On behalf of the Subcommittee on Biorheology of the Scientific and Standardization Committee of the ISTH. Thromb Haemost 1996;76:118–123. [PubMed: 8819263]
3. Cantón G, Levy DI, Lasheras JC, Nelson PK. Flow changes caused by the sequential placement of stents across the neck of sidewall cerebral aneurysms. J Neurosurg 2005;103:891–902. [PubMed: 16304994]
4. Cebral JR, Castro MA, Burgess JE, Pergolizzi RS, Sheridan MJ, Putman CM. Characterization of cerebral aneurysms for assessing risk of rupture by using patient-specific computational hemodynamics models. AJNR Am J Neuroradiol 2005;26:2550–2559. [PubMed: 16286400]
5. Chiu JJ, Chen CN, Lee PL, Yang CT, Chuang HS, Chien S, Usami S. Analysis of the effect of disturbed flow on monocytic adhesion to endothelial cells. J Biomech 2003;36:1883–1895. [PubMed: 14614942]

6. Davies PF, Spaan JA, Krams R. Shear stress biology of the endothelium. Ann Biomed Eng 2005;33:1714–1718. [PubMed: 16389518]
7. Doerfler A, Wanke I, Egelhof T, Stolke D, Forsting M. Double-stent method: Therapeutic alternative for small wide-necked aneurysms. Technical note. J Neurosurg 2004;100:150–154. [PubMed: 14743929]
8. Garasic JM, Edelman ER, Squire JC, Seifert P, Williams MS, Rogers C. Stent and artery geometry determine intimal thickening independent of arterial injury. Circulation 2000;101:812–818. [PubMed: 10683357]
9. Hashimoto, S.; Manabe, S.; Matsumoto, Y.; Ikegami, K.; Tsuji, H.; Nakamura, T.; Murashige, Y.; Yamanaka, A.; Sakaue, K.; Kawamasa, T.; Kaku, S.; Otani, H.; Imamura, H. The effect of pulsatile shear flow on thrombus formation and hemolysis. Presented at the 22nd Annual Engineering in Medicine and Biology Society International Conference; July 23–28, 2000; Chicago, IL.
10. Hashimoto S, Nishiguchi K, Abe Y, Nie M, Takayana T, Asari H, Kazama S, Ishihara A, Sasada T. Thrombus formation under pulsatile flow: Effect of periodically fluctuating shear rate. Jpn J Artif Organs 1990;19:1207–1210.
11. Hashimoto T, Meng H, Young WL. Intracranial aneurysms: Links among inflammation, hemodynamics and vascular remodeling. Neurol Res 2006;28:372–380. [PubMed: 16759441]
12. Hinds MT, Park YJ, Jones SA, Giddens DP, Alevriadou BR. Local hemodynamics affect monocytic cell adhesion to a three-dimensional flow model coated with E-selectin. J Biomech 2001;34:95–103. [PubMed: 11425085]
13. Hoi Y, Meng H, Woodward SH, Bendok BR, Hanel RA, Guterman LR, Hopkins LN. Effects of arterial geometry on aneurysm growth: Three-dimensional computational fluid dynamics study. J Neurosurg 2004;101:676–681. [PubMed: 15481725]
14. Howington JU, Hanel RA, Harrigan MR, Levy EI, Guterman LR, Hopkins LN. The Neuroform stent, the first microcatheter-delivered stent for use in the intracranial circulation. Neurosurgery 2004;54:2–5. [PubMed: 14683535]
15. Krings T, Hans FJ, Möller-Hartmann W, Brunn A, Thiex R, Schmitz-Rode T, Verken P, Scherer K, Dreeskamp H, Stein KP, Gilsbach J, Thron A. Treatment of experimentally induced aneurysms with stents. Neurosurgery 2005;56:1347–1360. [PubMed: 15918952]
16. Lanzino G, Wakhloo AK, Fessler RD, Hartney ML, Guterman LR, Hopkins LN. Efficacy and current limitations of intravascular stents for intracranial internal carotid, vertebral, and basilar artery aneurysms. J Neurosurg 1999;91:538–546. [PubMed: 10507372]
17. Liou TM, Liou SN. Pulsatile flows in a lateral aneurysm anchored on a stented and curved parent vessel. Exp Mech 2004;44:253–260.
18. Lopes DK, Ringer AJ, Boulos AS, Qureshi AI, Lieber BB, Guterman LR, Hopkins LN. Fate of branch arteries after intracranial stenting. Neurosurgery 2003;52:1275–1279. [PubMed: 12762872]
19. Malek AM, Alper SL, Izumo S. Hemodynamic shear stress and its role in atherosclerosis. JAMA 1999;282:2035–2042. [PubMed: 10591386]
20. Masuda H, Zhuang YJ, Singh TM, Kawamura K, Murakami M, Zarins CK, Glagov S. Adaptive remodeling of internal elastic lamina and endothelial lining during flow-induced arterial enlargement. Arterioscler Thromb Vasc Biol 1999;19:2298–2307. [PubMed: 10521357]
21. Meng H, Swartz DD, Wang Z, Hoi Y, Kolega J, Metaxa EM, Szymanski MP, Yamamoto J, Sauvageau E, Levy EI. A model system for mapping vascular responses to complex hemodynamics at arterial bifurcations in vivo. Neurosurgery 2006;59:1094–1100. [PubMed: 17143243]
22. Sani S, Lopes DK. Treatment of a middle cerebral artery bifurcation aneurysm using a double neuroform stent “Y” configuration and coil embolization: Technical case report. Neurosurgery 2005;57:E209. [PubMed: 15987593]
23. Sho E, Sho M, Hoshina K, Kimura H, Nakahashi TK, Dalman RL. Hemodynamic forces regulate mural macrophage infiltration in experimental aortic aneurysms. Exp Mol Pathol 2004;76:108–116. [PubMed: 15010288]
24. Shojima M, Oshima M, Takagi K, Torii R, Hayakawa M, Katada K, Morita A, Kirino T. Magnitude and role of wall shear stress on cerebral aneurysm: Computational fluid dynamic study of 20 middle cerebral artery aneurysms. Stroke 2004;35:2500–2505. [PubMed: 15514200]

25. Tanishita, K.; Ohmura, H.; Ueda, A.; Kudo, S.; Tateshhima, S.; Ikeda, M. Frontiers of bio-fluid mechanics and mass transfer in the arterial system. Presented at the 6th World Conference on Experimental Heat Transfer, Fluid Mechanics, and Thermodynamics; April 17–21, 2005; Matsushima, Miyagi, Japan.

26. Tzima E, Del Pozo MA, Kiosses WB, Mohamed SA, Li S, Chien S, Schwartz MA. Activation of Rac1 by shear stress in endothelial cells mediates both cytoskeletal reorganization and effects on gene expression. EMBO J 2002;21:6791–6800. [PubMed: 12486000]

27. Ujiie H, Tachibana H, Hiramatsu O, Hazel AL, Matsumoto T, Ogasawara Y, Nakajima H, Hori T, Takakura K, Kajiya F. Effects of size and shape (aspect ratio) on the hemodynamics of saccular aneurysms: A possible index for surgical treatment of intracranial aneurysms. Neurosurgery 1999;45:119–130. [PubMed: 10414574]

34. Ujiie H, Tamano Y, Sasaki K, Hori T. Is the aspect ratio a reliable index for predicting the rupture of a saccular aneurysm? Neurosurgery 2001;48:495–503. [PubMed: 11270538]

29. Vanninen R, Manninen H, Ronkainen A. Broad-based intracranial aneurysms: Thrombosis induced by stent placement. AJNR Am J Neuroradiol 2003;24:263–266. [PubMed: 12591645]

30. Wanke I, Doerfler A, Schoch B, Stolke D, Forsting M. Treatment of wide-necked intracranial aneurysms with a self-expanding stent system: Initial clinical experience. AJNR Am J Neuroradiol 2003;24:1192–1199. [PubMed: 12812954]

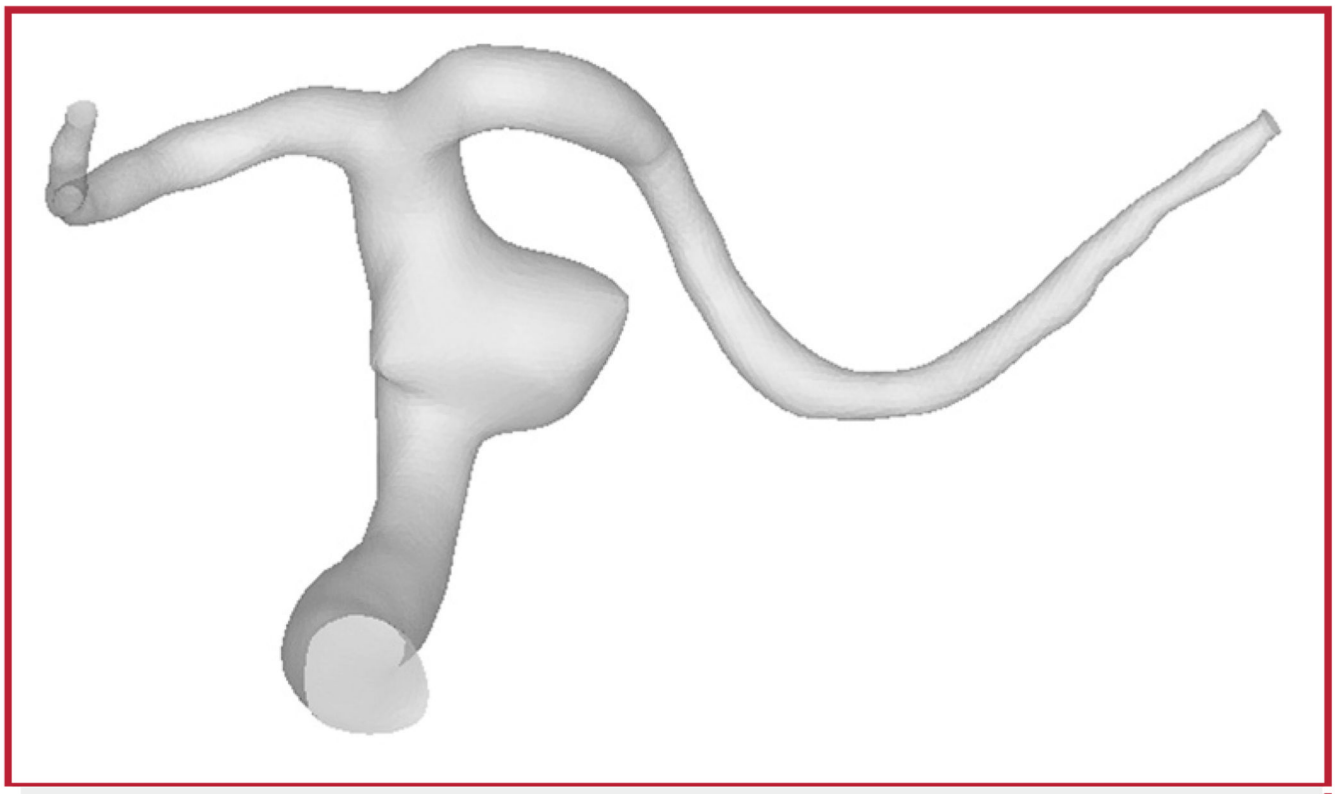

Figure 1.
Geometry of a basilar artery saccular aneurysm and parent artery reconstructed from a patient's computed tomographic angiography images.

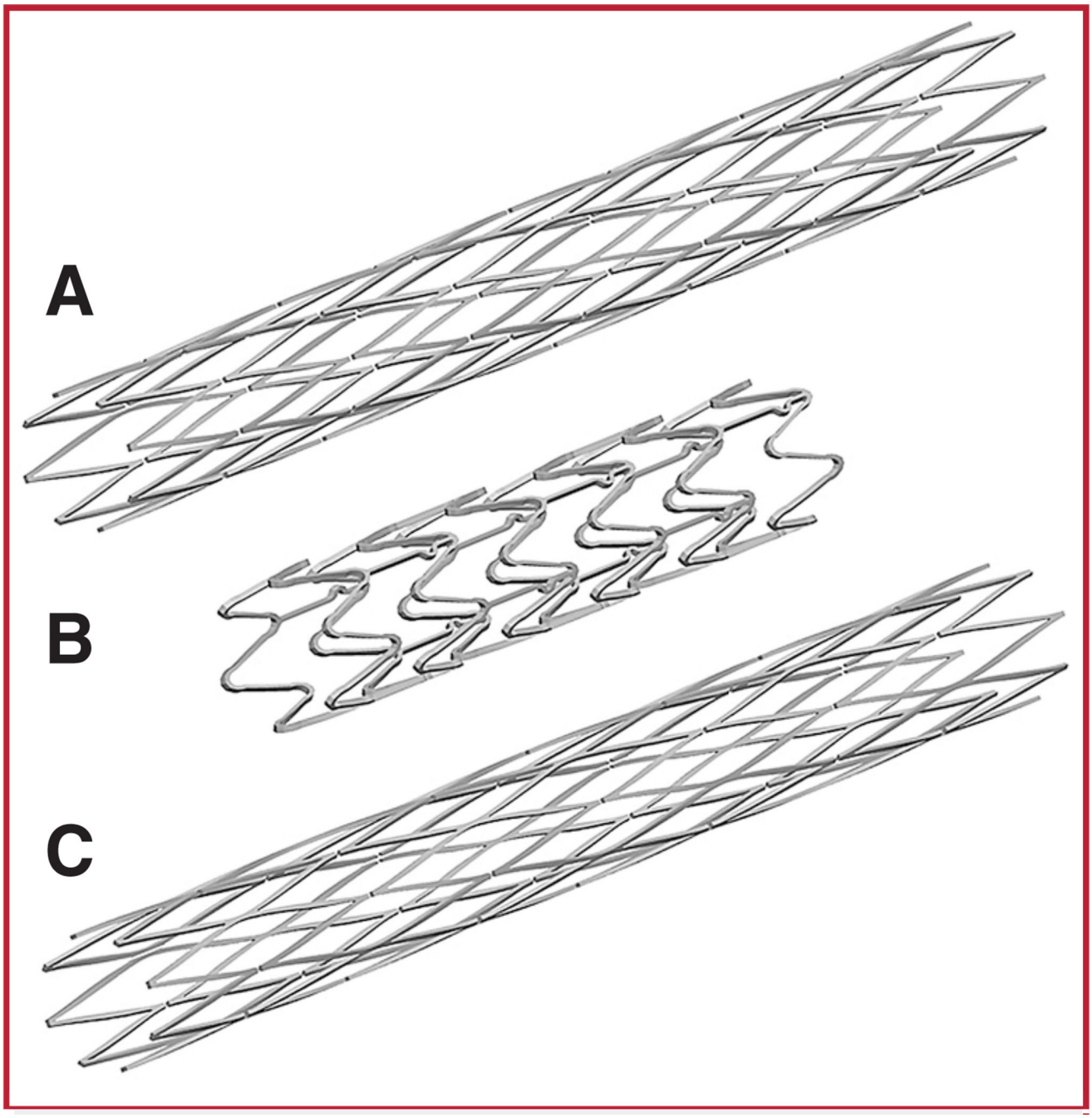

Figure 2.
Reconstructed geometries of the stents. *A*, Neuroform2; *B*, Vision; and *C*, Wingspan.

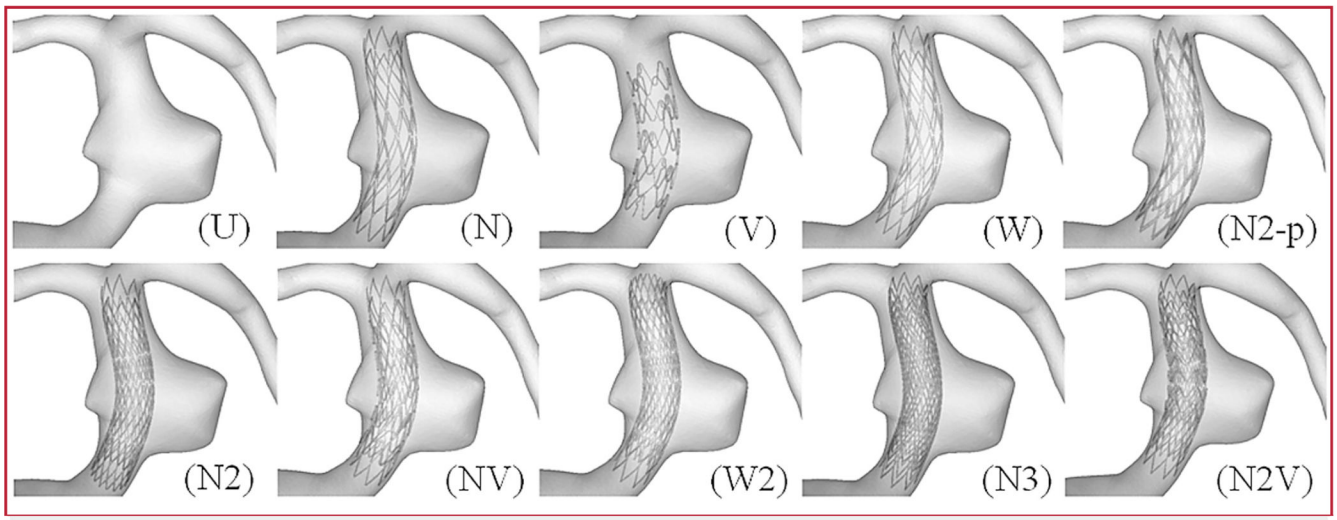

Figure 3.
Geometries of the aneurysm models. *U*, unstented; *N*, Neuroform2; *V*, Vision; *W*, Wingspan; N2-p, poor deployment double-Neuroform2; *N2*, double-stent using Neuroform2; *NV*, double-stent using Neuroform2 and Vision; *W2*, double-stent using Wingspan; *N3*, triple-stent using Neuroform2; *N2V*, triple-stent using two Neuroform2 stents and one Vision stent.

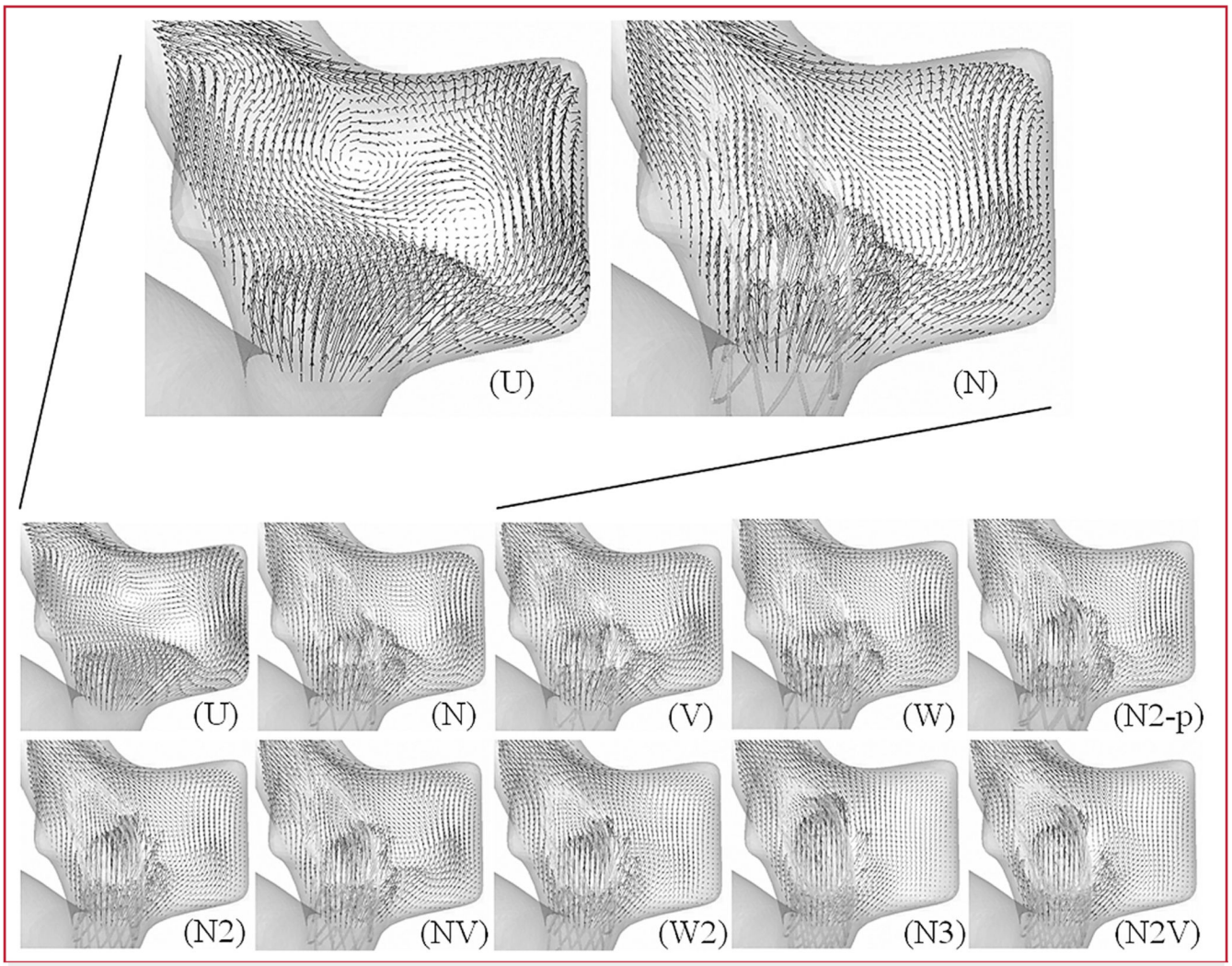

Figure 4.
Aneurysmal flow patterns on a midplane of the aneurysm. *U*, unstented; *N*, Neuroform2; *V*, Vision; *W*, Wingspan; N2-p, poor deployment double-Neuroform2; *N2*, double-stent using Neuroform2; *NV*, double-stent using Neuroform2 and Vision; *W2*, double-stent using Wingspan; *N3*, triple-stent using Neuroform2; *N2V*, triple-stent using two Neuroform2 stents and one Vision stent.

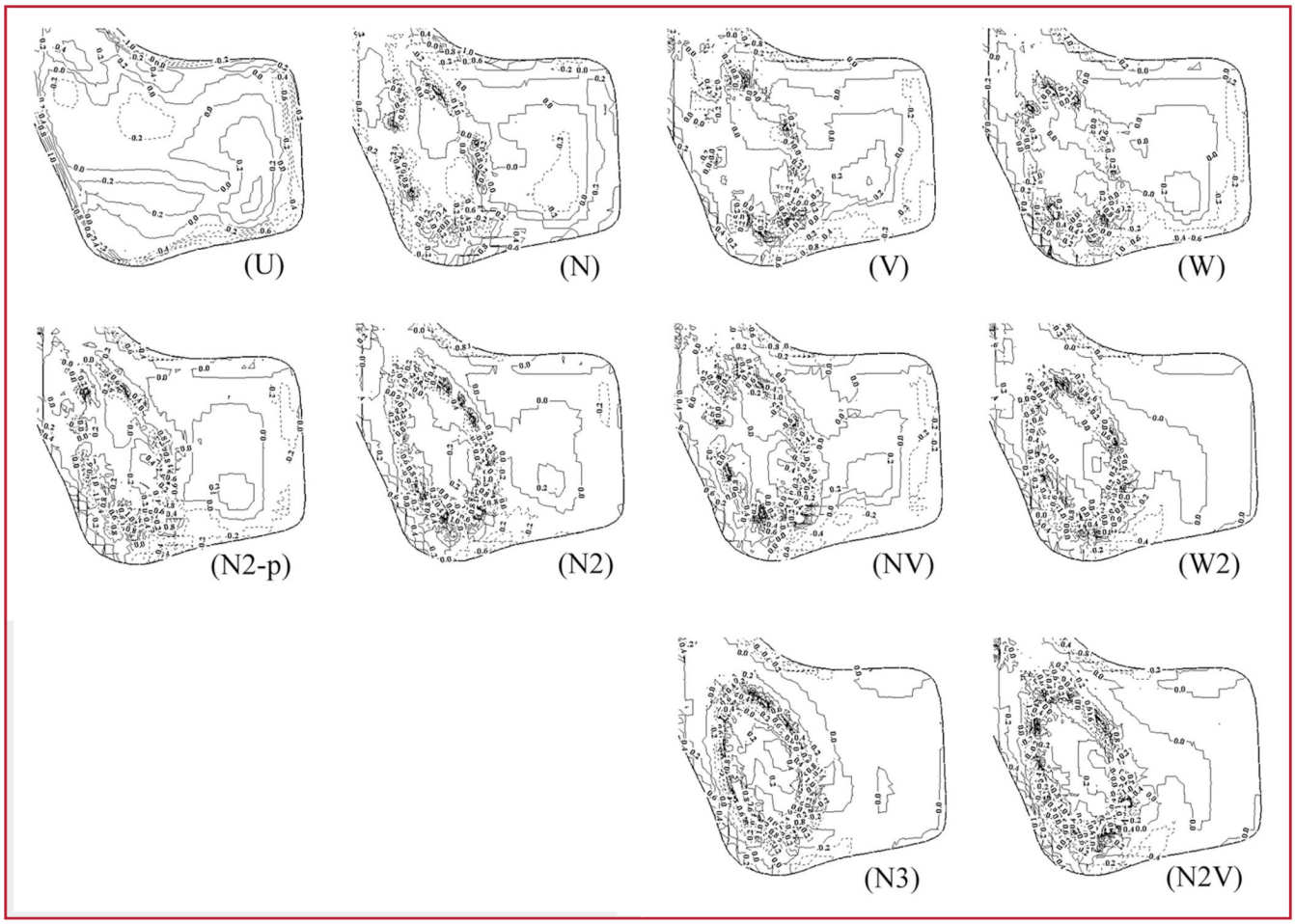

Figure 5.

Average out-of-plane vorticity in the dome of the aneurysm models. *U*, unstented; *N*, Neuroform2; *V*, Vision; *W*, Wingspan; N2-p, poor deployment double-Neuroform2; *N2*, double-stent using Neuroform2; *NV*, double-stent using Neuroform2 and Vision; *W2*, double-stent using Wingspan; *N3*, triple-stent using Neuroform2; *N2V*, triple-stent using two Neuroform2 stents and one Vision stent.

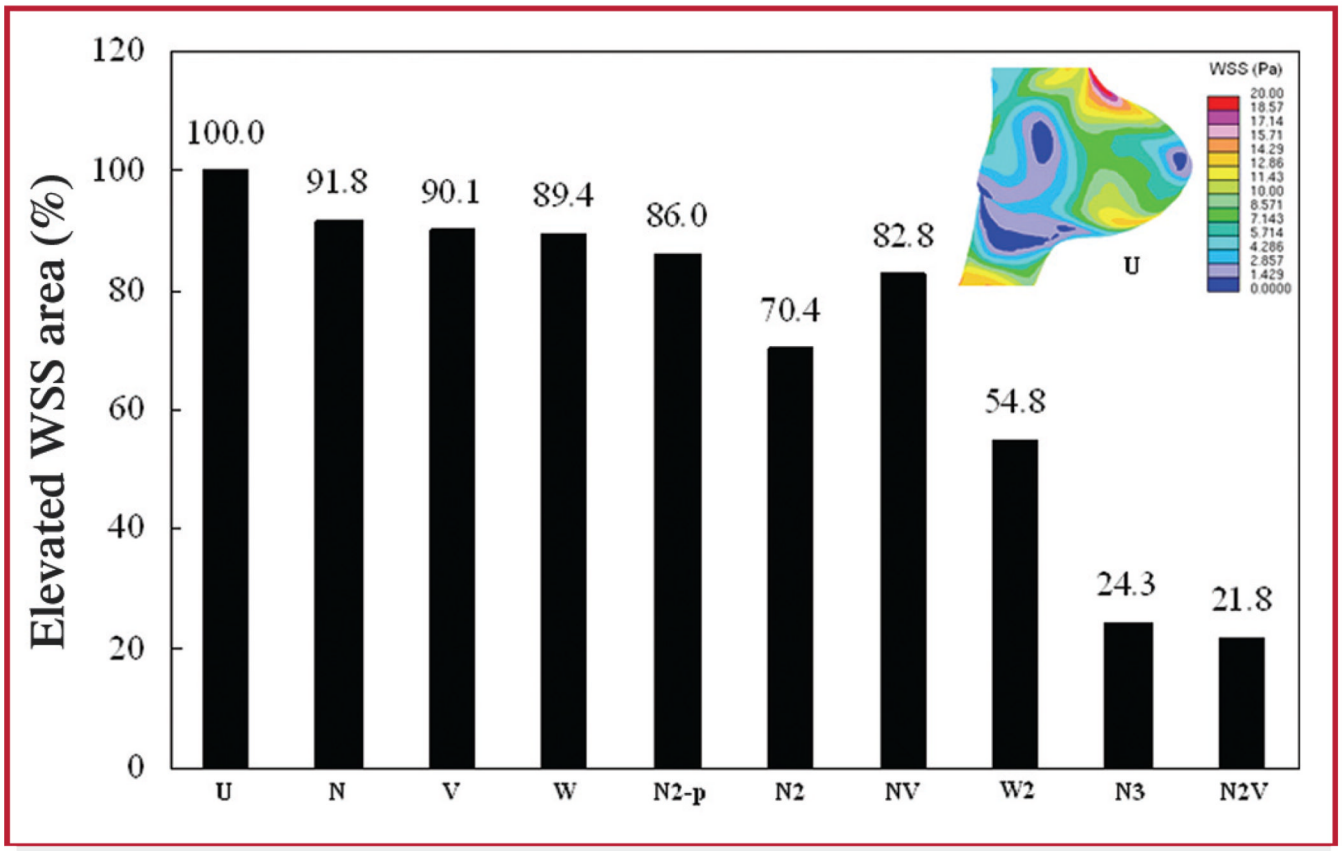

Figure 6.
Elevated wall shear stress areas (in percent) in the aneurysm. *U*, unstented; *N*, Neuroform2; *V*, Vision; *W*, Wingspan; N2-p, poor deployment double-Neuroform2; *N2*, double-stent using Neuroform2; *NV*, double-stent using Neuroform2 and Vision; *W2*, double-stent using Wingspan; *N3*, triple-stent using Neuroform2; *N2V*, triple-stent using two Neuroform2 stents and one Vision stent. For example, the colored inset shows WSS distribution of the unstented aneurysm model.

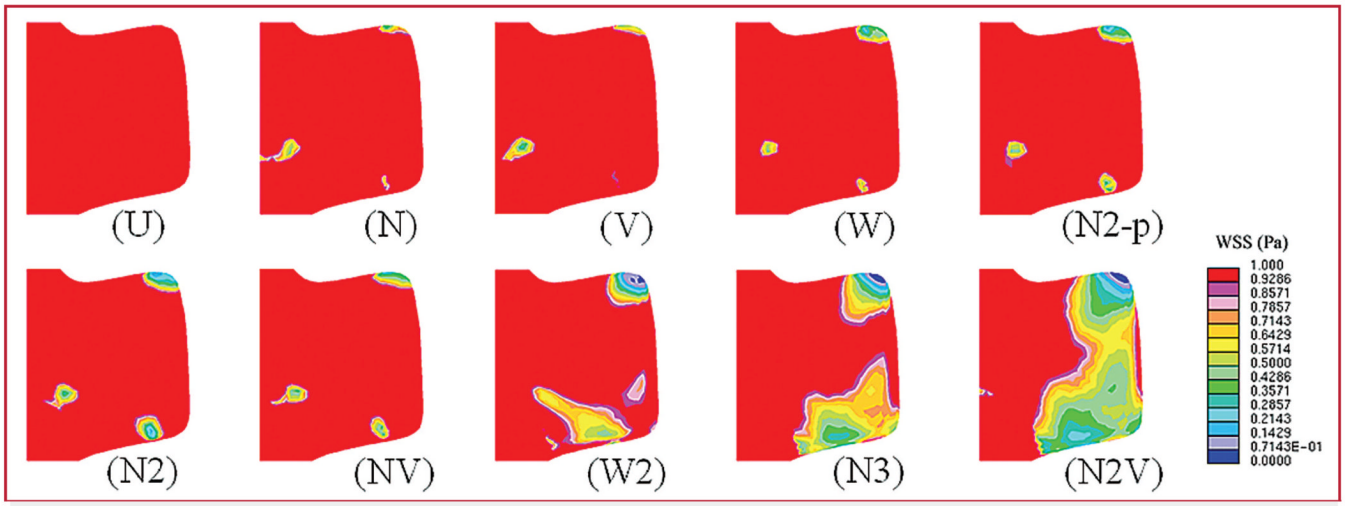

Figure 7.

Examples of low-level wall shear stress (*WSS*, in Pascals [*P*a]) in the aneurysm models. *U*, unstented; *N*, Neuroform2; *V*, Vision; *W*, Wingspan; N2-p, poor deployment double-Neuroform2; *N2*, double-stent using Neuroform2; *NV*, double-stent using Neuroform2 and Vision; *W2*, double-stent using Wingspan; *N3*, triple-stent using Neuroform2; *N2V*, triple-stent using two Neuroform2 stents and one Vision stent.

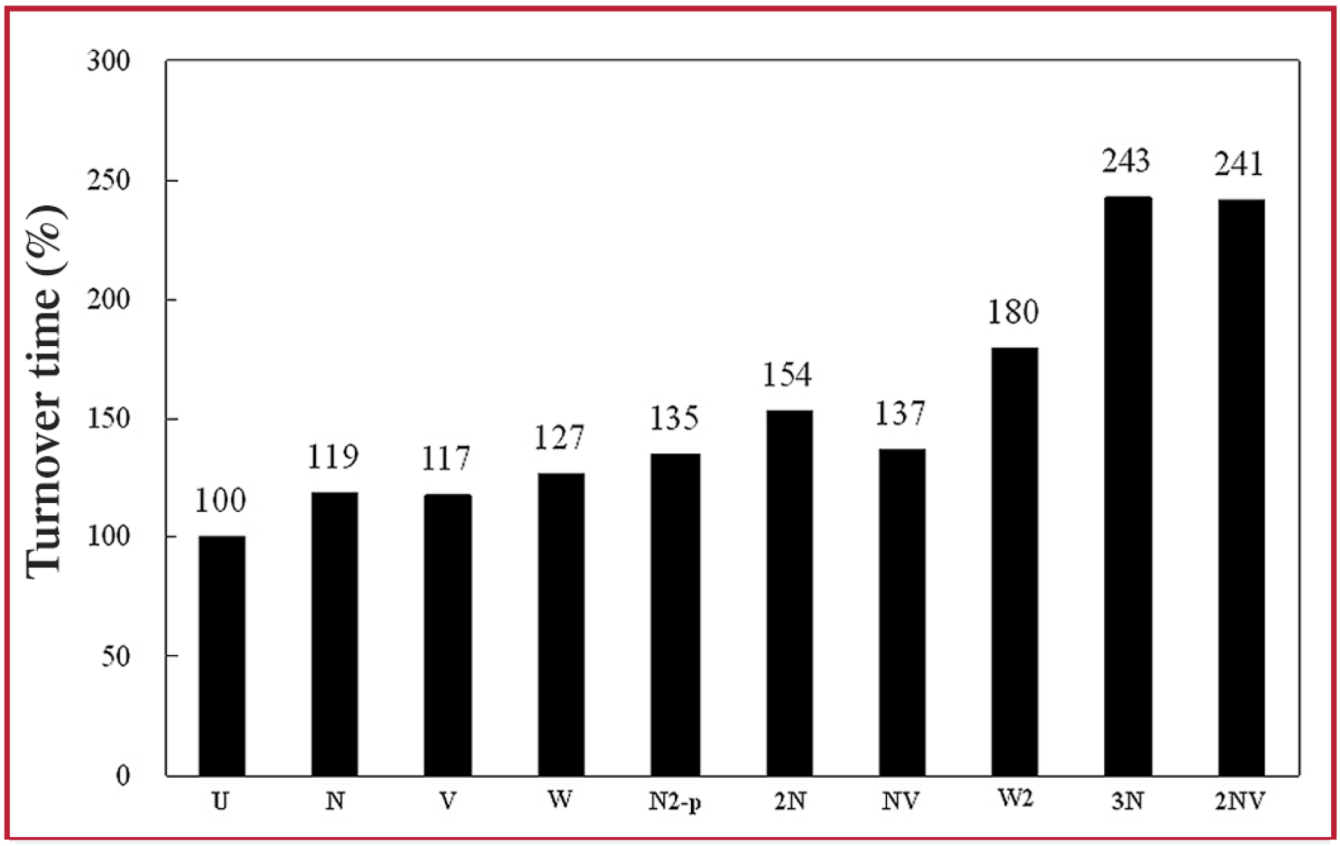

Figure 8.
Aneurysm turnover times (in percent) in the aneurysm models. *U*, unstented; *N*, Neuroform2; *V*, Vision; *W*, Wingspan; N2-p, poor deployment double-Neuroform2; *N2*, double-stent using Neuroform2; *NV*, double-stent using Neuroform2 and Vision; *W2*, double-stent using Wingspan; *N3*, triple-stent using Neuroform2; *N2V*, triple-stent using two Neuroform2 stents and one Vision stent.

TABLE 1

Unstented and stented aneurysm models

Sequence	Model	Model description
Single stent	U	Unstented
—	N	Neuroform2 stent
—	V	Vision stent
—	W	Wingspan stent
Double stent[a]	N2-p	Two poorly deployed Neuroform2 stents
—	N2	Two Neuroform2 stents
—	NV	One Neuroform2 stent and one Vision stent
—	W2	Two Wingspan stents
Triple stent[a]	N3	Three Neuroform2 stents
—	N2V	Two Neuroform2 stents and one Vision stent

[a]For multiple-stented aneurysm models, each additional stent was angularly and longitudinally shifted from the previous stent position to equally divide the existing porous space so as to minimize the flow permeability of the stent combinations. In the N2-p case (two poorly deployed Neuroform2 stents), the stents were placed very close to each other by minimal shifting of the second stent from the first one.